Int. J. Electrochem. Sci., 15 **(2020)** 6217 – 6226, doi: 10.20964/2020.07.66

International Journal of
ELECTROCHEMICAL
SCIENCE
www.electrochemsci.org

High Rate Performance of Pd-doped $Li_3V_2(PO_4)_3$/C Cathode Materials Synthesized via Controllable Sol-Gel Method

Yu Zhang

College of pharmacy, Xinjiang Medical University, Urumqi, 830011 Xinjiang, China
E-mail: 270478879@qq.com

Received: 8 March 2020 / *Accepted:* 2 May 2020 / *Published:* 10 June 2020

Li-ion batteries play a significant role in new energy source development, which focuses on obtaining the best cathode material. Here, electrode materials with different palladium content (x = 0, 0.01, 0.05, and 0.09) were synthesized via the sol-gel method. The microstructure and morphology were characterized by X-ray diffraction and transmission electron microscopy. The electrochemical properties of as-prepared samples were measured by constant current tests. The experimental results suggested that appropriate Pd doping can't increase the performance of the materials obviously under the condition of low rate, but can significantly improve the rate capabilities of $Li_3V_2(PO_4)_3$/C cathodes at high rate. The sample with the best electrochemical performance was doped to x=0.05. The first-discharge capacity reached 111.9 $mAh \cdot g^{-1}$ at 5 C in the potential range of 2–4.3 V. After the different rates cycle-life process, the initial discharge retention was 95.7%, exhibiting excellent rate capability and stability.

Keywords: $Li_3V_{2-x}Pd_x(PO_4)_3$/C; sol-gel method; rate performance; electrochemical performance

1. INTRODUCTION

As the economy continues to grow, the demand for energy is increasing. New, reusable lithium-ion batteries play an important role in the development and application of new energy sources, and thus have become a focus for research[1-3]. Efficient and stable cathode materials are key to promoting further growth in lithium-ion batteries[4-6]. Among currently used cathode materials, polyanionic $Li_3V_2(PO_4)_3$ has many advantages because of its structure, such as high discharge capacity and stability during electrochemical performance. This has attracted attention from many researchers. It has a three-dimensional network structure material formed by sharing oxygen atom vertices between VO_6 octahedron and PO_4 tetrahedron units. However, this structure also means that the metal atoms are separated by oxygen atoms, which leads to a lower conductivity and rate performance, limiting the applications of $Li_3V_2(PO_4)_3$ cathode materials[7, 8]. According to the literature, there are many ways to overcome these shortcomings. The most common methods are to coat the cathode with conductive

materials or introduce additional cations or anions by doping. At present, the reported cations used for doping are K^+[9], Na^+[10], Co^{2+}[11], Mn^{2+}[12], Mg^{2+}[13], Ni^{2+}[14], Cr^{3+}[15], Fe^{3+}[16], Y^{3+}[17], Ge^{4+}[18], Ti^{4+}[19], and Nb^{5+}[20], among others. They can affect the electronic conductivity and rate capability of cathode materials to varying degrees, improving the overall performance. Interestingly, due to its excellent electrical conductivity, ductility, catalysis, and thermal stability, Pd is widely used in materials, mechanics, thermodynamics, catalysts, and other industrial fields. However, whether its special properties can have a positive effect on the electrochemical performance of $Li_3V_2(PO_4)_3$ has not yet been systematically reported. Therefore, this paper focuses on the effect of doping with Pd on the electrochemical properties of $Li_3V_2(PO_4)_3$.

In this paper, a series of Pd-doped $Li_3V_2(PO_4)_3$ materials were synthesized by the sol-gel method, and the morphology and electrochemical properties of the materials were investigated. Through this exploration, the results show that this modified method has indeed improved the electrochemical properties of $Li_3V_2(PO_4)_3$, and greatly improved the conductivity and rate capability of the sample. The optimum doping amount was found to be x = 0.05.

2. EXPERIMENTAL DETAILS

The $Li_3V_{2-x}Pd_x(PO_4)_3/C$ (x=0, 0.01, 0.05 and 0.09) cathode materials were synthesized by a controlled sol-gel method. The initial materials $CH_3COOLi{\cdot}2H_2O$, V_2O_5, $PdCl_2$, H_3PO_4, and citric acid were mixed together in a molar ratio of 3.15:(1-0.5x):x:3:(1-0.5x) (x=0, 0.01, 0.05 and 0.09). First, V_2O_5 was dissolved into the appropriate amount of H_2O_2 until the solution became transparent. Then, $CH_3COOLi{\cdot}2H_2O$ was added to the solution to form solution A. Next, $PdCl_2$ was dissolve in 2 mL of concentrated hydrochloric acid under constant ultrasound until it became transparent solution B, and B was then added to solution A to form solution C. H_3PO_4 and citric acid were then simultaneously dissolved in 60 mL of deionized water until they became transparent solution D. Finally, D was slowly added to C and stirred continuously by a magnet for 2 h, as the solution changed color from orange to green. The green solution was dried at 90 ℃ for 12 h in a dry box to form a green solid. The solid was ground into powder, which was then presintered at 350 ℃ for 4 h and sintered at 800 ℃ for 12 h in a tube furnace with flowing Ar_2. A sample of the active material was recovered after the powder returned to room temperature and was ground.

The as-prepared samples were tested by X-ray diffraction (XRD, Bruker D2) using Cu K-α radiation. The morphology of the material was characterized by transmission electron microscopy (TEM, Philips CM10). The electronic states of the elements were assessed by X-ray photoelectron spectroscopy (XPS, ESCALAB 250Xi).

The electrodes were obtained by mixing the active material, acetylene black, and polytetrafluoroethylene (PTFE) in a weight ratio of 80:15:5. The mixed slurry was evenly coated on aluminum foil, then dried at room temperature and cut into circles with 10 mm diameters, which were dried under vacuum (110 °C for 12 h). Li wafers were used for the anode, $Li_3V_{2-x}Pd_x(PO_4)_3/C$ for the cathode, polypropylene/polyethylene/polypropylene (PP/PE/PP) composite film for the separator, and 1 M $LiPF_6$ dissolved in a mixture of ethylene carbonate and dimethyl carbonate (1:1 by volume) for the

electrolyte. Finally, two-electrode electrochemical cells were assembled in an argon-filled glove box. The cycle lives of the cells were evaluated with a battery test instrument (LAND, CT-2001A) at different rates (0.2, 0.5, 1, 2, and 5 C) in the voltage range from 2 to 4.3 V. Cyclic voltammetry (CV) and electrochemical impedance spectroscopy (EIS) measurements were obtained using an electrochemical workstation (LK2005A) after the cycling tests. The CV tests were done after 150 weeks of cycling at a scanning rate of 0.1 $mV \cdot s^{-1}$ in the potential range from 2 to 4.3 V.

3. RESULTS AND DISCUSSION

The XRD profiles of the $Li_3V_{2-x}Pd_x(PO_4)_3/C$ composites are shown in Fig.1 (a). The doping amount is listed on the top right of each diffraction curve. The XRD patterns show the same peaks for the doped and pure materials, and they are all indexed as monoclinic structures, which is consistent with previous studies[21-23]. At the same time, no impurity diffraction peaks are found, illustrating that the prepared materials are single-phase, and the carbon coated on the surface of the material is amorphous [24, 25]. In order to further explore the chemical composition and state of the synthetic material, the valence states of each element in the material were characterized by XPS survey spectra. Fig.1 (b) and (c) are enlarged diagrams of XPS survey spectra of $Li_3V_{2-x}Pd_x(PO_4)_3/C$ (x = 0.05) material over the range from 512 to 528 eV and 332 to 346 eV, respectively. It can be seen from Fig.1 (b) that there are two apparent peaks at binding energies of 517.08 and 524.08 eV corresponding to V $2p_{3/2}$ and V $2p_{1/2}$, respectively[26-28], This indicates that the valence of the vanadium ions in the sample is +3. In addition, from Fig.1 (c), there are two clear peaks in binding energy at 336.08 and 341.38 eV corresponding to Pd $3d_{5/2}$ and Pd $3d_{3/2}$ orbital energies, respectively, which is consistent with measurements for PdO. This suggests that the valence state of Pd in the material is +2 and that Pd^{2+} ions are successfully doped into the $Li_3V_2(PO_4)_3$ material.

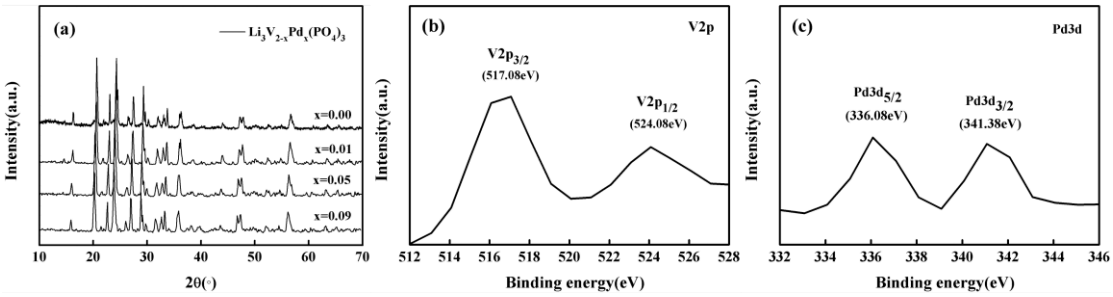

Figure 1. (a) XRD profiles of $Li_3V_{2-x}Pd_x(PO_4)_3/C$ (x=0, 0.01, 0.05, 0.09) composites, and enlarged XPS survey spectra for the $Li_3V_{2-x}Pd_x(PO_4)_3/C$ sample (x = 0.05) from (b) 512 to 528 eV and (c) 332 to 346 eV.

Fig.2 shows the high resolution (HR) TEM image of $Li_3V_{1.95}Pd_{0.05}(PO_4)_3/C$. Fig.2 (a) has a unit size of 50 nm, and (b) has a unit size of 5 nm. Fig.2 (a) shows that particles synthesized in this study are spherical, with a size distribution range from 50 to 200 nm. Spherical particles can effectively increase the surface area of the material and the contact area between the composite and electrolyte, enhancing

the ionic conductivity and contributing to superior electrochemical performance in the electrode. High-power TEM analysis of $Li_3V_{1.95}Pd_{0.05}(PO_4)_3/C$ is shown in Fig.2 (b), and lattice fringes can be clearly observed in the picture. The lattice spacing of 0.33 nm determined by TEM corresponds to the diffraction peak of the (1 3 1) plane, which is further proof that the synthesized sample is of a pure phase[29]. Through the above experimental results of XRD, XPS and TEM, it can be shown that $Li_3V_{2-x}Pd_x(PO_4)_3/C$ materials were successfully synthesized. Moreover, a layer of carbon film is coated uniformly on the surface of the material, which will help to raise the electronic conductivity and discharge capacity of the sample[24, 25]. An elemental analysis test result shows that the carbon content of the $Li_3V_{1.95}Pd_{0.05}(PO_4)_3/C$ composite is 3.6%.

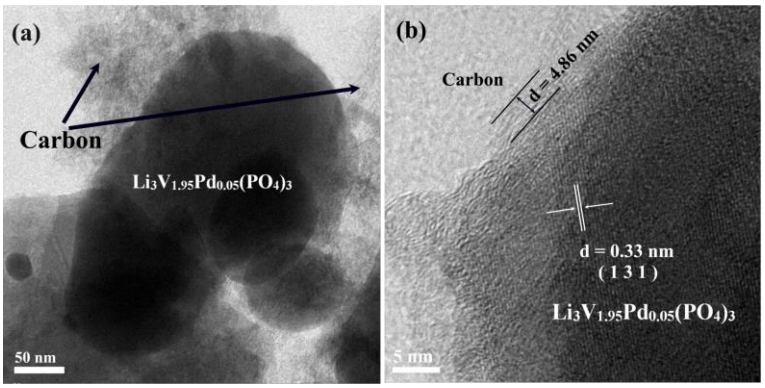

Figure 2. HRTEM images of an as-prepared sample of $Li_3V_{1.95}Pd_{0.05}(PO_4)_3/C$ with a unit size of (a) 50 nm and (b) 5 nm.

The electrochemical properties of $Li_3V_{2-x}Pd_x(PO_4)_3/C$ (x = 0.00, 0.01, 0.05, 0.09) were investigated using a constant current test. Fig.3 shows the charge-discharge curves for the composites at rate of 0.2 C between 2 and 4.3 V. Curves a, b, c, and d represent materials doped with Pd^{2+} in amounts of x = 0, x = 0.01, x = 0.05 and x = 0.09, respectively. During the charging and discharging process, phase transitions occur with the extraction and insertion of Li^+. In the charge-discharge voltage range from 3 to 4.8 V, three Li^+ from $Li_3V_2(PO_4)_3$ will be separated in four steps during the charging process, corresponding to four phase transitions of $Li_3V_2(PO_4)_3$ to $Li_{2.5}V_2(PO_4)_3$, $Li_{2.5}V_2(PO_4)_3$ to $Li_2V_2(PO_4)_3$, $Li_2V_2(PO_4)_3$ to $LiV_2(PO_4)_3$, and $LiV_2(PO_4)_3$ to $V_2(PO_4)_3$[30]. That is to say, three lithium ions in the material can be completely deblocking, corresponding to four pairs of redox peaks. When the potential range is controlled within 2 to 4.3 V, we can see that there are three clear sets of charge-discharge platforms in the curve of pure $Li_3V_2(PO_4)_3/C$, which indicate the processes of embedding and releasing two Li^+ from the electrode. It is clear that the modified materials in b, c, and d consist of two sets of charging and discharging platforms. By careful comparison, it can be found that the first charging platforms of the three doped materials occur at a lower potential, and by increasing the doping amount, the platforms decrease further. Meanwhile, the second charging platforms occur at higher potentials. This is because the valence of Pd^{2+} is lower than that of V^{3+}. The introduction of low-valence ions reduces the initial charging platforms of materials. With the release of Li^+ during the charging process, in order to compensate for the loss of charged materials, more low-valence V^{3+} will be converted to high-valence states, resulting in higher-valence phases, and increasing the potential of the second charging

platform. This is also the reason why the first and second discharging platforms of the doped materials are elevated with respect to the pure material. Some platforms overlap because of the decrease or increase in charging and discharging platforms. Therefore, as shown in the figure, the charge-discharge platforms of doped materials have changed from three sets to approximately two.

The specific discharge capacities of the electrodes with doping of palladium (x = 0, 0.01, 0.05, and 0.09) are 127.9, 130.1, 133.6, and 118.4 mAh·g^{-1}, respectively, at a charging rate of 0.2 C and in the voltage range from 2 to 4.3 V. Clearly, doping with Pd can improve the discharge capacity of the $Li_3V_2(PO_4)_3$/C material, except for the sample with doping of x = 0.09. This is because Pd itself has no electrochemical activity, so excessive doping causes the active material content in the electrode to decrease, thus reducing the discharge capacity of the material. Therefore, when the material is doped to x=0.05, the discharge capacity of the material is highest.

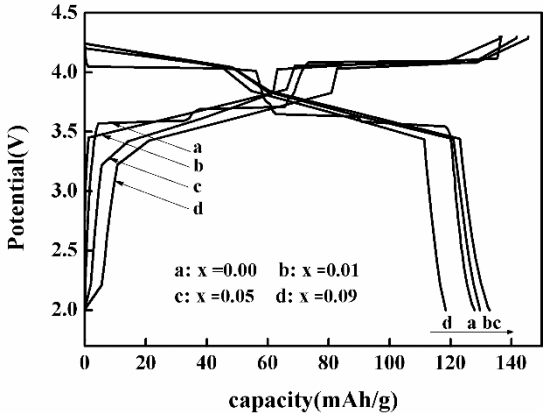

Figure 3. The first charge-discharge curves of $Li_3V_{2-x}Pd_x(PO_4)_3$/C (x=0, 0.01, 0.05, 0.09) composites.

Rate capability is an important part of the study of electrochemical properties. Cycle life diagrams of the materials at various rates are shown in Fig.4. From this information the discharge capacities and high-rate discharge capacity retentions (HRDCR) were determined and are listed in Table 1 for comparison. From the data in the table, it can be seen that the first-discharge capacities of the pure material are 127.9 mAh·g^{-1} at 0.2 C and 60.1 mAh·g^{-1} at 5 C, in the voltage range from 2 to 4.3 V. A high specific-discharge capacity is exhibited by the pure material, which is similar to its theoretical capacity at 0.2 C. However, as the rate increased, the capacity decayed rapidly. When the rate is 5 C, the HRDCR of the pure material is only 48.1%. In Pd^{2+}-doped $Li_3V_2(PO_4)_3$/C at x=0.01, 0.05, and 0.09, the specific-discharge capacities are 130.1, 133.6, 118.4 mAh·g^{-1} at 0.2 C and 98.0, 111.9, 90.1 mAh·g^{-1} at 5 C, respectively. Additionally, the HRDCR of the doped materials are 75.3, 83.8 and 76.1%, respectively. The HRDCR of $Li_3V_{1.95}Pd_{0.05}(PO_4)_3$/C is 1.74 times that of the pure material. When the material is doped to x = 0.05, the sample has the highest rate capability. After 150 cycles, when the rate decreases to 0.2 C, the discharge capacity of $Li_3V_{1.95}Pd_{0.05}(PO_4)_3$/C electrodes can still reach 127.9 mAh·g^{-1}, and the initial capacity retention rate is 95.7%, delivering a high rate capability and cycling performance.

Table 2 is the comparison of high-rate discharge capacity retentions of materials doped with different cations. In general, the influence of doping different ions on the properties of materials is

different. Since the radius, charge, doping amount and electrochemical activity of the ion all may be the factors to enhance or inhibit the performance of materials, which constitute a comprehensive mechanism. For the cathode material of lithium-ion battery, the introduction of foreign ions can release a higher capacity under the conditions of larger charge-discharge rate and lower charge-discharge potential, which is a better improvement of its rate performance. Because this can allow the battery to finish the charge-discharge process in a short time and obtain higher energy. By comparing the data in Table 1 and table 2, It can be seen that the introduction of appropriate Pd ions, in the condition of low rate, does not significantly improve the performance of the material, but in the condition of high rate, it shows an advantage. Under the condition of high rate, it has a high capacity retention rate. The introduction of Pd can greatly improve the high rate performance and stability of the material. This is because Pd itself has no electrochemical activity, but it has a special and stable electronic structure. The introduction of an appropriate amount of Pd can effectively reduce the degree of ordering in the lattice and maintain stability in the crystal structure, thus enhancing the rate capability and stability of the material.

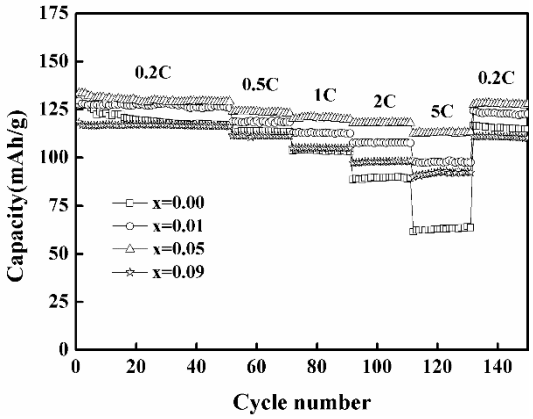

Figure 4. Discharge performance of $Li_3V_{2-x}Pd_x(PO_4)_3/C$ (x = 0, 0.01, 0.05, 0.09) composites at various cycling rates (0.2, 0.5, 1, 2, and 5 C) between 2 and 4.3 V.

Table 1. Comparison of discharge capacities and HRDCR of synthesized materials at different rates in the voltage range from 2 to 4.3 V .

Sample	Special-discharge capacity ($mAh \cdot g^{-1}$)					HRDCR (%)
	0.2 C	0.5 C	1 C	2 C	5 C	
$Li_3V_2(PO_4)_3/C$	127.9	112.8	103.6	88.5	61.5	48.1
$Li_3V_{1.99}Pd_{0.01}(PO_4)_3/C$	130.1	118.7	112.8	107.6	98.0	75.3
$Li_3V_{1.95}Pd_{0.05}(PO_4)_3/C$	133.6	120.5	118.0	115.9	111.9	83.8
$Li_3V_{1.91}Pd_{0.09}(PO_4)_3/C$	118.4	111.5	105.2	97.3	90.1	76.1

Table 2. Comparison of high-rate discharge capacity retentions of materials doped with different cations under various charge-discharge potentials.

Sample	Charge-discharge rate (C)	Special-discharge capacity (mAh·g^{-1})	HRDCR (%)	Reference
$Li_{2.97}Na_{0.03}V_2(PO_4)_3/C$	0.2	169.5	70.1	[10]
	2.0	118.9		
$Li_3V_{1.95}Mn_{0.05}(PO_4)_3/C$	0.1	180.0	57.8	[12]
	1.0	104.0		
$Li_3V_{1.9}Cr_{0.1}(PO_4)_3/C$	0.2	171.4	76.0	[15]
	4.0	130.2		
$Li_3V_{1.97}Y_{0.03}(PO_4)_3/C$	0.5	124.0	88.7	[17]
	1.5	110.0		
$Li_3V_{1.95}Pd_{0.05}(PO_4)_3/C$	0.2	133.6	83.8	This work
	5.0	111.9		

The extraction/insertion mechanism of Li^+ and the reversibility of the materials were investigated by CV. As shown by the peaks in Fig.5, all the materials have the same Li extraction/insertion mechanism. There are three sets of redox peaks, corresponding to three redox processes. This is consistent with the results obtained from the charge-discharge capacity tests for the first cycle of the materials. The inset in Fig.5 shows an in-depth comparison of CV curves located in the range from approximately 3.8 to 4.3 V. It can be seen that after different rate cycling processes, compared to $Li_3V_2(PO_4)_3/C$ electrode, the doped materials peaks are sharper and have higher peak current values. As shown in Table 2, the difference between oxidation and reduction voltages for curves a, b, c, and d is 0.149, 0.119, 0.117, and 0.141 V, respectively. It is well known that the smaller the difference between the oxidation peak and the reduction peak voltage of the material, the better the reversibility of the material. From these results, we can deduce that these electrode materials show enhanced reversibility when doped with Pd, and the best doping amount is x = 0.05.

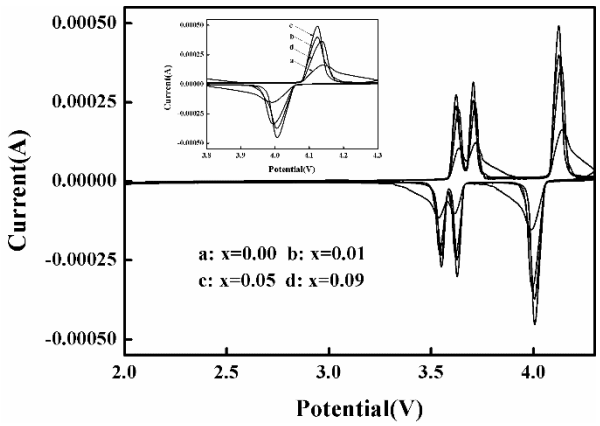

Figure 5. CV curves of $Li_3V_{2-x}Pd_x(PO_4)_3/C$ (x = 0, 0.01, 0.05, 0.09) composites in the potential range 2-4.3V with a scan rate of 0.1 mV s^{-1} after 150 cycles.

Table 3. Redox peak voltage and the corresponding voltage differences for $Li_3V_{2-x}Pd_x(PO_4)_3/C$ materials in the voltage range from 3.8 to 4.3 V.

Sample	Opv (V)	Rpv (V)	ΔV (V)
$Li_3V_2(PO_4)_3/C$	4.140	3.991	0.149
$Li_3V_{1.99}Pd_{0.01}(PO_4)_3/C$	4.124	4.005	0.119
$Li_3V_{1.95}Pd_{0.05}(PO_4)_3/C$	4.124	4.007	0.117
$Li_3V_{1.91}Pd_{0.09}(PO_4)_3/C$	4.136	3.995	0.141

Opv: oxidation peak voltage; Rpv: Reduction peak voltage; ΔV: redox voltage difference.

In order to further explore the internal electrochemical mechanisms of Pd-doped electrodes, the electrochemical testing was carried out by EIS after 150 cycles in the potential range from 2 to 4.3 V (as shown in Fig.6 (a)). It can be seen from Fig.6 (a) that the materials all give approximately the same Nyquist diagram, which is consists of a small intercept, a semi-circle, and an oblique line. These components represent uncompensated resistance (R_e), charge transfer resistance (R_{ct}), and Li^+ diffusion in the electrode (W_s), respectively[31-33]. Fig.6 (b) shows the relationship between Z_{re} and ($\omega^{-1/2}$) in the low-frequency region. The inset in Fig.6 (a) shows an equivalent circuit used to fit the experimental data, and the fitting results of the equivalent circuit and the Li-ion diffusion coefficient data are calculated and listed in Table 3 [34, 35]. The results show that Pd doping can tremendously reduce the charge transfer impedance and effectively improve the Li^+ mobility in materials. This is conducive to promoting the electrochemical properties of electrodes, especially critical factors which improve the rate performance of the material. However, Pd doping does not act on all $Li_3V_2(PO_4)_3/C$ materials in the same way, but rather acts along a parabolic trend. When the doping amount is small, it has a negligible effect on the materials, while excessive doping will reduce the amount of active ingredients in the sample.

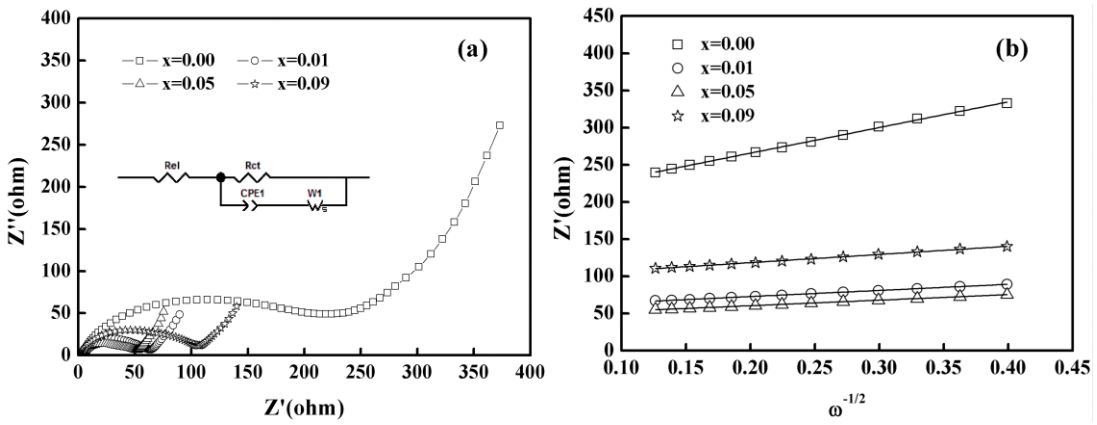

Figure 6. (a) Nyquist plots from the EIS of $Li_3V_{2-x}Pd_x(PO_4)_3/C$ (x=0, 0.01, 0.05, 0.09) materials; (b) the relationship between Z_{re} and $\omega^{-1/2}$ at low frequencies.

Therefore, it will affect the crystal structure of the materials and cause adverse effects on the

compounds. When the doping amount is x = 0.05, the $Li_3V_{1.95}Pd_{0.05}(PO_4)_3$/C material has the smallest charge transfer impedance and largest Li-ion diffusivity, showing that proper doping can effectively improve the electrochemical properties of materials, which is consistent with the above electrochemical test results.

Table 4. Kinetic parameters of $Li_3V_{2-x}Pd_x(PO_4)_3$/C electrodes obtained from equivalent circuit fitting of experimental data.

Sample	R_e (Ω)	R_{ct} (Ω)	D ($cm^2 \cdot s^{-1}$)
$Li_3V_2(PO_4)_3$/C	3.24	220.80	3.30×10^{-12}
$Li_3V_{1.99}Pd_{0.01}(PO_4)_3$/C	2.83	57.01	5.19×10^{-11}
$Li_3V_{1.95}Pd_{0.05}(PO_4)_3$/C	2.76	47.27	6.30×10^{-11}
$Li_3V_{1.91}Pd_{0.09}(PO_4)_3$/C	2.37	114.10	2.97×10^{-11}

R_e: uncompensated resistance; R_{ct}: charge transfer resistance; D: Li diffusion coefficient.

4. CONCLUSIONS

In this study, $Li_3V_{2-x}Pd_x(PO_4)_3$/C materials were successfully prepared by the controllable sol-gel method. TEM images show that the material produced forms spherical particles of uneven size, in a distribution between 50 and 200 nm. Electrochemical data for the $Li_3V_{2-x}Pd_x(PO_4)_3$/C materials were obtained from a series of electrochemical tests. Through comparison, the positive effects of adding Pd into $Li_3V_2(PO_4)_3$/C on its rate performance and stability were determined. Doping with the proper amount of Pd can effectively prevent rapid attenuation of the capacity of the material under high rate conditions. When the material is doped to x = 0.05, the material exhibits the best electrochemical performance. In the voltage range from 2 to 4.3 V, the $Li_3V_{1.95}Pd_{0.05}(PO_4)_3$/C material displays specific-discharge capacities of 133.6 $mAh \cdot g^{-1}$ at 0.2 C and 111.9 $mAh \cdot g^{-1}$ at 5 C. The high rate capacity retention is 83.8%, which surpasses many cationic modification methods currently reported. After 150 cycles with different rates, the rate changed from 5 C to 0.2 C, and a favorable discharge capacity could still be obtained. The initial capacity retention rate can reach 95.7%, showing good chemical stability.

ACKNOWLEGEMENTS

This study was supported by Natural Science Foundation of Xinjiang Uygur Autonomous Region (2017D01C231).

References

1. B. Scrosati, J. Hassoun and Y.K. Sun, *Energy Environ. Sci.*, 4 (2011) 3287.
2. L.X. Yuan, Z.H. Wang, W.X. Zhang, X.L. Hu, J.T. Chen, Y.H. Huang and J.B. Goodenough, *Energy*

Environ. Sci., 4 (2011) 269.
3. G.E. Blomgren, *J. Electrochem. Soc.*, 164 (2017) A5019.
4. K.J. Stevenson, *J. Solid State Electrochem.*, 16 (2012) 2017.
5. Y.P. Wu, E. Rahm and R. Holze, *J. Power Sources*, 114 (2003) 228.
6. H. Kim, M.Z. Kong, K. Kim, I. Kim and H. Gu, *J. Power Sources*, 171 (2007) 917.
7. Y.X. Liao, C. Li, X.B. Lou, X.S. Hu, Y.Q. Ning, F.Y. Yuan, B. Chen, M. Shen and B.W. Hu, *Electrochim. Acta*, 271 (2018) 608.
8. Z.Q. Cao, C.Y. Zuo, X.M. Cui and X.F. Zhang, *Ionics*, 25 (2019) 1.
9. L. Jiang, C.P. Fu, K.Q. Li, H.H. Zhou,Y.P. Huang and Y.F. Kuang, *Mater. Lett.*, 198 (2017) 73.
10. M.M. Jia, Y.H. Zhang, H.L. Tian and Z. Su, *Int. J. Energy Res.*, 43 (2019) 6004.
11. M.M. Ren, M.Z. Yang, W.L. Liu, M. Li, L.W. Su, X.B. Wang and Y.H. Wang, *J. Power Sources*, 326 (2016) 313.
12. J.S. Park, J. Kim, W.B. Park, Y.K. Sun and S.T. Myung, *ACS Appl. Mater. Interfaces*, 9 (2017) 40307.
13. Y.Z. Dong, Y.M. Zhao and H. Duan, *J. Electroanal. Chem.*, 660 (2011) 14.
14. M. Choi, H.S. Kim, Y.M. Lee and B.S. Jin, *Mater. Lett.*, 145 (2015) 83.
15. Y.H. Chen, Y.M. Zhao, X.N. An, J.M. Liu, Y.Z. Dong and L. Chen, *Electrochim. Acta*, 54 (2009) 5844.
16. Y. Kee, N. Dimov, E. Kobayashi, A. Kitajou and S. Okada, *Solid State Ionics*, 272 (2015) 138.
17. S.K. Zhong, L.T. Liu, J.Q. Jiang, Y.W. Li, J. Wang, J.Q. Liu and Y.H. Li, *J. Rare Earths*, 27 (2009) 134.
18. Y. Zhang, Z. Su and J. Ding, *J. Alloys Compd.*, 702 (2017) 427.
19. S.K. Zhong ,Y. Wang, L. Wu and J.Q. Liu, *Rare Met.*, 8 (2015) 286.
20. Y. Xia, W.K. Zhang, H. Huang, Y.P. Gan, C.G. Li and X.Y. Tao, *Mater. Sci. Eng. B*, 176 (2011) 633.
21. A.V. Ivanishchev, A.V. Ushakov, I.A. Ivanishcheva, A.V. Churikov, A.V. Mironov, S.S. Fedotov, N.R. Khasanova and E.V. Antipov, *Electrochim. Acta*, 230 (2017) 479.
22. Y. Xia, S. Shi, C.G. Li, C. Liang, Y.P. Gan, H. Huang, X.Y. Tao and W.K. Zhang, *J. Alloys Compd.*, 652 (2015) 298.
23. Y.X. Liao, C. Li, X.B Lou, X.S. Hu, Y.Q. Ning, F.Y. Yuan, B. Chen, M. Shen and B.W. Hu, *Electrochim. Acta*, 271 (2018) 608.
24. Y.Q. Qiao, X.L. Wang, J.Y. Xiang, D. Zhang, W.L. Liu and J.P. Tu, *Electrochim. Acta*, 56 (2011) 2269.
25. Q. Kuang and Y. Zhao, *J. Power Sources*, 216 (2012) 33.
26. G.L. Zeng, W. Zhou, J.L. Zheng, Z.H. Fan and H. Chen, *J. Nanosci. Nanotechnol.*, 20 (2020) 313.
27. M.M. Ren, Z. Zhou, Y.Z. Li, X.P. Gao and J. Yan, *J. Power Sources*, 162 (2006) 1357.
28. J.S. Huang, L. Yang and K.Y. Liu, *Mater. Chem. and Phys*, 128 (2011) 470.
29. X.H. Rui, N. Ding, J. Liu, J. Liu, C. Li and C.H. Chen, *Electrochim. Acta*, 55 (2010) 2384.
30. M. Secchiarolia, R. Marassi, M. Wohlfahrt-Mehrens and S. Dsoke, *Electrochim. Acta*, 219 (2016) 425.
31. Y.C. Si, Z. Su, Y.B. Wang and T. Ma, *New J. Chem.*, 39 (2015) 8971.
32. Y.S. Hu, X. Ma, P. Guo, F. Jaeger and Z.H. Wang, *J. Alloys and Compd.*, 723 (2017) 873.
33. Z. Li, L.L. Zhang, X.L. Yang, H.B. Sun, Y.H. Huang and G. Liang, *RSC Adv.*, 6 (2016) 10334.
34. Q. Liu, L.B. Ren, C.J. Cong, F. Ding, F.X. Guo, D.W. Song, J. Guo, X.X. Shi and L.Q. Zhang, *Electrochim. Acta*, 187 (2016) 264.
35. Y. Xia. W.K. Zhang, H. Huang, Y.P. Gan, C.G. Li and X.Y. Tao, *Mater. Sci. Eng. B*, 176 (2011) 633.